

# Robust adaptive integral sliding mode control of a half-bridge bidirectional DC-DC converter

Julius Derghe Cham<sup>1</sup>, Francis Lénine Djanna Koffi<sup>1</sup>, Alexandre Teplaira Boum<sup>2</sup>, Ambe Harrison<sup>3</sup>

<sup>1</sup>Technology and Applied Sciences Laboratory, University of Douala, Douala, Cameroon

<sup>2</sup>Department of Electrical and Electronics Engineering, ENSET, University of Douala, Douala, Cameroon

<sup>3</sup>Department of Electrical and Electronics Engineering, College of Technology, University of Buea, Buea, Cameroon

## Article Info

### Article history:

Received May 14, 2024

Revised Sep 13, 2024

Accepted Oct 1, 2024

### Keywords:

Adaptive integral sliding mode controller

Bidirectional DC-DC converter

Boost mode

Buck mode

Integral sliding mode control

Particle swarm optimization

Robust controller

## ABSTRACT

A novel approach to improving the dynamic response of a half-bridge bidirectional DC-DC converter is presented in this paper, particularly in the face of disturbances from internal or external sources. These converters, which are integral to the operation of DC microgrids, are responsible for stepping up or stepping down voltage as required. To optimize the converter's performance under varying conditions, we propose an adaptive integral sliding mode controller (AISMIC) enhanced by particle swarm optimization (PSO). The proposed controller leverages the strengths of both super-twisting sliding mode control (STSMC) and adaptive control, providing a robust and responsive solution to the challenges posed by the converter's nonlinear dynamics. The system's stability is rigorously ensured through the application of Lyapunov stability criteria, which underpin the enhanced performance of the controller. Simulations conducted in the MATLAB/Simulink environment demonstrate that the AISMICPSO outperforms conventional control strategies, offering superior stability, robustness, and precision. The results clearly indicate that the proposed approach minimizes errors and enhances the overall efficiency and reliability of the bidirectional half-bridge DC-DC converter, making it a highly effective solution for DC microgrid applications.

This is an open access article under the [CC BY-SA](https://creativecommons.org/licenses/by-sa/4.0/) license.



## Corresponding Author:

Julius Derghe Cham

Technology and Applied Sciences Laboratory, University of Douala

P.O. Box, 7236 Douala, Cameroon

Email: julius.cham@yahoo.com

## 1. INTRODUCTION

Bidirectional DC-DC converters have been essential in recent times for controlling and stabilizing DC bus voltage in a range of applications, including microgrids, distributed generating systems, energy storage systems, electric cars, power filters, and solar or wind energy systems [1], [2]. In DC microgrids, DC-DC converters are used to raise or lower the energy produced, which typically does not match the demands of the load [3], [4]. A DC-DC converter functioning in bidirectional mode enhances the efficiency and performance of DC microgrids by serving as an interface between a power source and a storage unit [5]. Notwithstanding the significant role that two-way DC-DC converters play in the aforementioned applications, a number of researchers have focused on their control due to various issues, including voltage ripple, output-tracking performance that is susceptible to time-varying system parametric uncertainties, nonlinear properties, and mismatched and matched disturbances that require attention [6]. A suitable control strategy will help solve some of these challenges and ensure the efficient performance of the system [3]. Because of their versatility and ease of use, proportional-integral (PI) and proportional-integral-derivative

(PID) controllers are frequently utilized in the control of DC-DC converters working in bidirectional mode. They are limited when it comes to working with nonlinear systems. However, lengthy settling times, significant overshoot, and a lack of robustness in the face of parameter variations are typically the main features of results obtained with such controllers [2], [7]–[11]. Pany *et al.* [12] and Cheng *et al.* [13] have done some work on the linear control of bidirectional DC-DC converters. Although these suggested controllers achieved their design goals, they still have certain shortcomings, including poor performance during parameter fluctuations, extended settling and rising periods, overshoot, and resilience. DC-DC converters working in bidirectional mode are better when using nonlinear controllers. Many studies have been done on the sliding mode control (SMC) of DC-DC converters running in bidirectional mode, and the results obtained met the objectives for which they were designed. However, numerous works are presented in the literature to address some of the problems posed by the nonlinearity of the half-bridge bidirectional DC-DC converters studied in these papers. One of the most exploited controllers is the SMC, despite the problem of chattering with it. The efficacy of this approach can be attributed to its nonlinear features, great stability, ease of implementation, resilience, and insensitivity to perturbations [14] and [15]. Moreover, due to the nonlinearity property of bidirectional DC-DC converters, linear control techniques cannot cope with this type of system, leading to some limitations, such as large voltage disturbances [16]. Despite the good control qualities of SMC, there are still some issues with this control technique that need to be handled. The chattering effect, poor performance under significant load and parameter fluctuations, and the existence of steady-state flaws in the regulation are a few of these difficulties [1]. Researchers have suggested various control strategies to manage the bidirectional half-bridge DC-DC converters in an effort to address some of these issues. Numerous solutions are available in the literature to address some of the problems with SMC that are shown in [7], [15], [17]–[20]. In order to guarantee stability, quick reaction times, and steady state properties, [2], [13] created a few control strategies with acceptable outcomes. In their simulated results, it is evident that the proposed controllers performed better than the existing ones in terms of stabilization and reference tracking under load resistance variations, input voltage variation, and Buck-boost mode switching of a DC-DC converter working in bidirectional mode. However, there are still several problems with the aforementioned control strategies, including the complexity of the design, the necessity for precise selection of the adaptive gains, and the need for further steady state error reduction.

The paper addresses the significant challenges in controlling half-bridge DC-DC converters working in bidirectional mode, which are crucial in applications such as DC microgrids, energy storage systems, and electric vehicles. These converters manage the bidirectional flow of energy, stepping up or stepping down voltages as needed. However, their nonlinear behavior and sensitivity to disturbances, such as input voltage fluctuations and load variations, create substantial control difficulties. Traditional controllers, like PI and PID controllers, are commonly used due to their simplicity but have notable limitations when applied to these converters. PI and PID controllers often struggle with slow settling times, where the system takes longer to stabilize after a disturbance. They are also prone to overshoot, where the output exceeds the desired value before settling, and lack robustness against parameter variations, meaning small changes in system parameters can lead to degraded performance or instability. These issues result in suboptimal performance, manifesting as voltage ripple, poor output tracking, and overall instability, which undermine the efficiency and reliability of the converters in dynamic environments. In high-demand applications like energy storage and electric vehicles, these performance shortcomings can lead to energy losses, reduced system efficiency, and even system failures. The paper highlights the need for more advanced control strategies that can overcome the limitations of traditional methods, ensuring higher efficiency, reliability, and stability in managing the complex dynamics of half-bridge bidirectional DC-DC converters.

To address these challenges, the paper proposes a robust adaptive integral sliding mode control (AISMC) approach enhanced by particle swarm optimization (PSO). This control strategy combines the advantages of adaptive sliding mode control with the robust nature of integral sliding mode control, while PSO is utilized to optimize the sliding coefficients dynamically. The AISMC is designed to adapt to changes in system dynamics, including load resistance variations and external disturbances, thereby improving the overall stability, accuracy, and performance of the DC-DC converter functioning in bidirectional mode. The proposed controller is validated through numerical simulations in a MATLAB/Simulink environment, which demonstrate its effectiveness in maintaining output voltage stability, reducing chattering phenomena, and minimizing steady-state errors compared to traditional control methods.

The results from the MATLAB/Simulink simulations reveal that the proposed AISMC outperforms conventional PI and standard integral sliding mode controllers (ISMC) across various scenarios, including input voltage disturbances, reference voltage changes, and load resistance variations. Notably, the AISMC achieves a significant reduction in the settling time, rise time, and undershoot in both step-up and step-down modes of operation. For instance, in buck mode, the AISMC reduced the settling time to 2.6 ms compared to 8.4 ms with the PI controller and minimized undershoot to 0.083% compared to 1.83% with the PI controller. In boost mode, the AISMC demonstrated similar improvements, with a settling time of 0.3 ms and an

undershoot of 0.041%. These results underscore the proposed controller's superior performance in enhancing the efficiency and reliability of half-bridge bidirectional DC-DC converters in dynamic and uncertain environments. As a result, the following can be used to summarize this paper's primary contributions:

- Development of a robust AISMC strategy: In this research, a novel control technique augmented by PSO that combines integral sliding mode control and adaptive sliding mode control is presented. By addressing nonlinear dynamics and disturbances in half-bridge bidirectional DC-DC converters, this solution offers enhanced stability, precision, and robustness in comparison to conventional control techniques.
- Optimization of sliding mode controller parameters: the use of PSO to dynamically optimize the sliding coefficients in the AISMC framework is a significant contribution. This optimization ensures that the controller can adapt to varying system conditions, such as changes in load resistance and input voltage, thereby maintaining optimal performance.
- Improvement in system efficiency and reliability: The proposed AISMC significantly enhances the efficiency and reliability of half-bridge bidirectional DC-DC converters, making them more suitable for dynamic and uncertain environments, such as those found in DC microgrids, energy storage systems, and electric vehicles.
- Reduction of chattering phenomena: The paper addresses the common issue of chattering in sliding mode controllers by integrating an adaptive mechanism that reduces oscillations and improves the smoothness of the control response, contributing to more stable and reliable converter operation.

## 2. METHOD

This paper employs a comprehensive and systematic approach to implementing an optimal control solution for a bidirectional half-bridge DC-DC converter. The methodology is meticulously structured and is visually represented in a block diagram in Figure 1, offering a clear and concise overview of the entire process. To ensure the robustness and effectiveness of the proposed control solutions, we utilize numerical simulations and implementations within the MATLAB/Simulink environment. This simulation platform provides a versatile and powerful toolset for modeling, analyzing, and optimizing complex control systems, allowing us to rigorously evaluate the performance of our proposed solutions under a variety of operating conditions. The process begins with a detailed mathematical modeling of the half-bridge converter, taking into account its distinct modes of operation—buck and boost modes. This modeling phase is critical, as it lays the foundation for understanding the system's dynamic behavior and identifying the key parameters that influence its performance. Following the modeling phase, we proceed to design the controllers for each mode of operation. These controllers are meticulously crafted to address the specific challenges connected with the nonlinear dynamics of the converter. The next step after design is optimization, when sophisticated methods like particle swarm optimization are used to adjust the controller parameters for best results. In the end, the regulated system is implemented in the MATLAB/Simulink environment where it is tested extensively under a range of conditions. These tests include variations in input voltage, load resistance, and reference voltage, allowing us to thoroughly investigate the system's stability, robustness, and overall performance across a wide range of scenarios. This methodical approach ensures that the proposed control solutions are not only theoretically sound but also practically viable, capable of delivering superior performance in real-world applications.

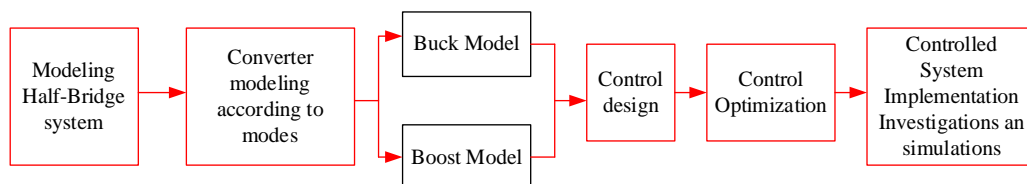


Figure 1. Comprehensive description of the study's methodology

Figure 2 provides a detailed illustration of the system under consideration, which comprises a bidirectional half-bridge DC-DC converter. This converter operates with an input voltage  $V_i$  and includes a battery that is modeled as an internal resistance, denoted as  $R_L$ . In this research,  $R_L$  is considered as the load when the converter is functioning in buck mode. The choice of the bidirectional half-bridge DC-DC converter is strategic due to its capability to efficiently manage the bidirectional flow of energy, making it ideal for applications such as DC microgrids and energy storage systems. The control strategy adopted for this converter is a combination of adaptive sliding mode control and PSO. This hybrid approach provides a

robust, efficient, and flexible control solution capable of handling dynamic changes within the system and mitigating external disturbances. The adaptive sliding mode control ensures that the controller can respond to abrupt variations in load resistance by dynamically adjusting the control parameters. The PSO algorithm further enhances this adaptability by optimizing the sliding mode controller's parameters in real-time, allowing the system to continuously adjust to shifts in operating conditions or environmental factors. The AISMC is designed to maintain optimal performance by continuously tuning these parameters, resulting in increased system efficiency and reduced oscillations, even under varying conditions. This approach ensures that the converter operates smoothly across its entire range of functions, providing reliable performance in both steady-state and transient conditions. Figures 2(a) and 2(b) show the schematic diagram of the system description and converter's topology that was chosen respectively. The two modes that govern this converter's operation are step-up, or boost mode, and step-down, or buck mode. The half-bridge bidirectional DC-DC converter (BDC) topology consists of a DC bus voltage  $V_i$  on the DC microgrid side,  $V_o$  is the output voltage on the energy storage unit side,  $C_A$  and  $C_B$  are capacitors on the DC microgrid side and energy storage unit side respectively,  $S_1$  and  $S_2$  are the upper and lower switches of the converter respectively.  $D_1$  and  $D_2$  are the diodes of the upper and lower switches of the converter, and  $L$  represents the inductor. The sophisticated control technique and extensive system design guarantee that the bidirectional half-bridge DC-DC converter performs well in a variety of settings, offering excellent performance and dependability in its intended use.

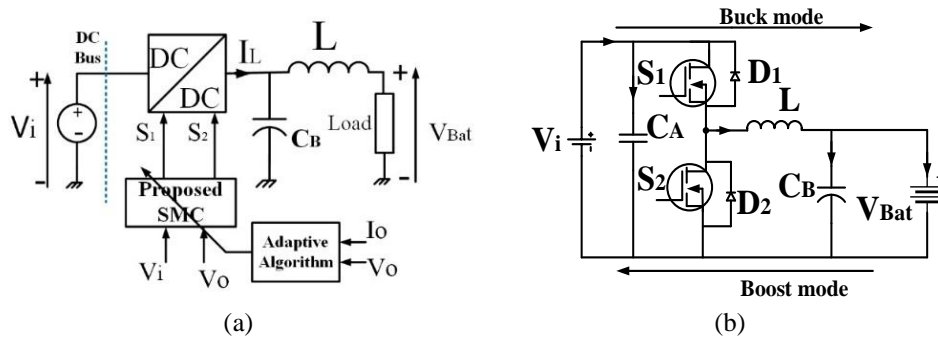


Figure 2. Schematic diagram of the system description (a) general schematic diagram and (b) half-bridge bidirectional DC-DC converter

### 2.1. Buck mode of operation

The topology of a bidirectional half-bridge DC-DC converter is chosen for this study because of the small current and voltage stresses of diodes and switching elements. Moreover, the existence of active components of small conduction loss as compared to other non-isolated bidirectional DC-DC converters [21]. The selected converter can be found in [21], [22]. This converter operates in two modes, i.e. buck and boost. The converter is made up of a DC bus voltage  $V_i$  on the DC microgrid side and an output voltage  $V_{Bat}$  on the battery side depending on the operating mode.  $C_A$  and  $C_B$  represent the capacitances of the capacitors connected in parallel to the grid and the battery respectively.  $S_1$  and  $S_2$  denote the converter's upper and lower switches respectively.  $D_1$  and  $D_2$  represent the diodes in parallel to the upper and lower switches of the converter respectively, and  $L$  denotes the inductor. In the buck mode of operation, power flows from the microgrid side to the load side. During this mode of operation, switch  $S_1$  and Diode  $D_2$  conduct while  $S_2$  and  $D_1$  are in OFF positions. Within this interval,  $S_1$  is ON while  $S_2$ ,  $D_1$  and  $D_2$  are turned OFF. The inductor  $L$  and Capacitor  $C_B$  are charged.  $D_2$  behaves as a freewheeling diode when  $S_1$  and  $S_2$  are turned OFF. To ease modeling, the battery is considered as an internal resistance. Equations (1) and (2) are derived from the application of Kirchhoff's current and voltage laws. The equivalent circuit of a half-bridge bidirectional DC-DC converter operating in step-down is illustrated in Figure 3. Figures 3(a) and 3(b) represent the equivalent circuit of the converter when the upper switch is on and off, respectively.

– Output equation when the upper switch is ON:

$$\begin{cases} \frac{dI_L}{dt} = \frac{V_{in} - V_{Bat}}{L} \\ \frac{dV_{C_B}}{dt} = \frac{I_L}{C_B} - \frac{V_{C_B}}{R_L C_2} \\ \frac{dV_{C_A}}{dt} = \frac{V_a - V_{C_A}}{r_1 C_A} - I_L \end{cases} \quad (1)$$

– Output equation when the lower switch is ON:

$$\begin{cases} \frac{dI_L}{dt} = -\frac{V_{CB}}{L} \\ \frac{dV_{CB}}{dt} = \frac{I_L}{C_B} - \frac{V_{CB}}{R_L C_B} \\ \frac{dV_{CA}}{dt} = \frac{V_a - V_{in}}{r_1 C_A} \end{cases} \quad (2)$$

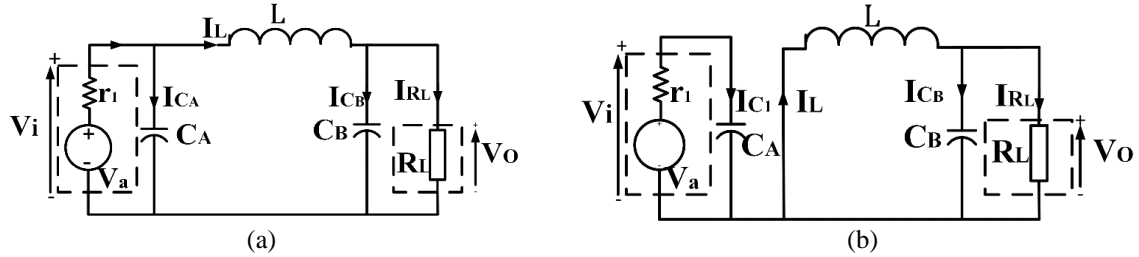


Figure 3. Equivalent circuit of half-bridge bidirectional DC-DC converter operating in buck mode (a) on state and (b) off state

**2.2. Boost mode of operation**

In the step-up mode of operation,  $S_2$  is turned ON and  $S_1$  remains OFF. The battery discharges thereby supplying the load with  $S_2$  and  $D_1$  conducting while  $S_1$  and  $D_2$  are turned OFF. During the first interval,  $S_2$  is turned ON with  $S_1$ ,  $D_1$ , and  $D_2$  maintained at OFF position. The inductor  $L$  and  $C_A$  are charged and no current flows through  $S_1$ . During the second interval,  $S_2$  and  $S_1$  are turned OFF, the circuit becomes an open circuit. The voltage across the inductor changes direction.  $D_1$  becomes forward biased and  $C_A$  is charged on a higher voltage than the input voltage. The circuit then operates in step-up mode. The following mathematical equations for the upper switch and lower switch on, respectively, may then be derived by using Kirchhoff's voltage law (KVL) and Kirchhoff's current law (KCL) in Figure 4. This leads us to (3) and (4). The corresponding circuit of the converter is shown in Figures 4(a) and 4(b) when the upper switch is turned on and off, respectively.

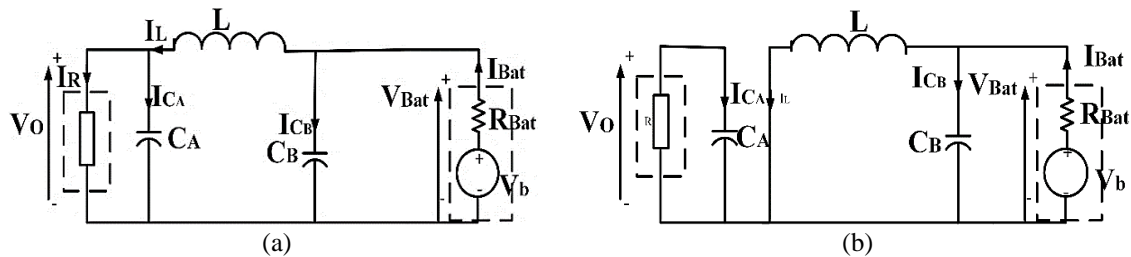


Figure 4. Equivalent circuit of a half-bridge bidirectional DC-DC converter operating in boost mode; (a) off state and (b) on state

– Output equation when the upper switch is ON

$$\begin{cases} \frac{dI_L}{dt} = \frac{-V_{CA} + V_{Bat}}{L} \\ \frac{dV_{CA}}{dt} = \frac{I_L}{C_A} - \frac{V_{CA}}{R C_A} \\ \frac{dV_{CB}}{dt} = \frac{V_{CB} - V_b}{r_2 C_B} - \frac{I_L}{C_B} \end{cases} \quad (3)$$

– Output equation when the lower switch is ON

$$\begin{cases} \frac{dI_L}{dt} = \frac{V_{Bat}}{L} \\ \frac{dV_{C_A}}{dt} = -\frac{V_O}{RC_A} \\ \frac{dV_{C_B}}{dt} = \frac{V_b - V_{Bat}}{r_2 C_B} - \frac{I_L}{C_B} \end{cases} \quad (4)$$

### 3. DESIGN OF NONLINEAR CONTROLLERS

#### 3.1. Design of integral sliding mode controller

In designing a sliding mode controller, one must first develop a state space equation for the system to be controlled as a function of the control variables [23]. It is then followed by designing a sliding surface, which leads to the derivation of a control law and ends by deriving the existing condition of the sliding mode controller [24]. To design the proposed controller for this system, we begin by designing an integral sliding mode controller with the converter operating in continuous conducting mode (CCM). The integral sliding mode control takes into consideration an additional voltage integral error term, which reduces the steady-state error of the conventional sliding mode controller [22].

##### 3.1.1. Buck mode

The ISMC design is quite different from the conventional SMC because it has three control parameters, which are the output voltage error  $y_1$ , the rate of change of the output voltage error  $y_2$ , and  $y_3$  is the integral of the output voltage error [25]. In each mode of operation, the control variable used is the output voltage  $V_{C_B}$  and  $V_{ref}$  signifies the desired value of the output voltage.

$$\text{Let } y_1 = V_{ref} - V_{C_B}, y_2 = \frac{V_{C_B}}{RLC_B} - \int \left( \frac{uV_i - V_{C_B}}{LC_B} \right) dt, \text{ and } y_3 = \int y_1 dt.$$

The state space equation with three control parameters ( $y_1, y_2, y_3$ ) can be expressed as in (5);

$$\begin{bmatrix} \dot{y}_1 \\ \dot{y}_2 \\ \dot{y}_3 \end{bmatrix} = \begin{bmatrix} 0 & 1 & 0 \\ 0 & \frac{1}{RLC_B} & 0 \\ 1 & 0 & 0 \end{bmatrix} \begin{bmatrix} y_1 \\ y_2 \\ y_3 \end{bmatrix} + \begin{bmatrix} 0 \\ -\frac{V_i}{LC_B} \\ 0 \end{bmatrix} u + \begin{bmatrix} 0 \\ \frac{V_{C_B}}{LC_B} \\ 0 \end{bmatrix} \quad (5)$$

$$u = \begin{cases} 1, \text{ when } S \geq 0 \\ 0, \text{ when } S < 0 \end{cases} \quad (6)$$

where  $u$  denotes the switch's switching state and  $V_i$  is the converter's input voltage. The general control law that is suitable for this system as adopted from reference [24] is given in (6).

The sliding surface can be defined in (7) as found in the following reference [25],

$$S_{buck} = \varphi_1 y_1 + \varphi_2 y_2 + \varphi_3 y_3 \quad (7)$$

$$\dot{S}_{buck} = \varphi_1 \dot{y}_1 + \varphi_2 \dot{y}_2 + \varphi_3 \dot{y}_3 \quad (8)$$

where  $\varphi_1, \varphi_2, \varphi_3$  are the sliding coefficients. The time derivative of  $S_{buck}$  is: To ensure the existence of sliding mode, the following inequality must be fulfilled:

$$S_{buck} \cdot \dot{S}_{buck} < 0 \quad (9)$$

From sliding mode's principle, when  $S_{buck} < 0, \dot{S}_{buck} > 0$  and  $u_{eq} = 0$ . When

$$S_{buck} > 0, \dot{S}_{buck} < 0 \text{ and } u_{eq} = 1 \quad (10)$$

$$0 < L \left( \frac{1}{RLC_B} - \frac{\varphi_1}{\varphi_2} \right) I_{C_B} + \frac{\varphi_3}{\varphi_2} (V_{ref} - V_{C_B}) LC_B + V_{C_B} < V_i \quad (11)$$

By solving  $\dot{S}_{buck} = 0$ , the equivalent control is obtained that is given in (12),

$$u_{eq} = \frac{L \left( \frac{1}{RLC_B} - \frac{\varphi_1}{\varphi_2} \right) I_{C_B} + \frac{\varphi_3}{\varphi_2} (V_{ref} - V_{C_B}) LC_B + V_{C_B}}{V_i} \quad (12)$$

$$0 < d = \frac{V_{\text{Control-signal}}}{V_{\text{saw-tooth}}} = \frac{V_c}{V_i} < 1 \quad (13)$$

where  $V_c$  signifies the control signal given in (14)

$$V_c = L \left( \frac{1}{R_L C_B} - \frac{\varphi_1}{\varphi_2} \right) I_{C_B} + \frac{\varphi_3}{\varphi_2} (V_{\text{ref}} - V_{C_B}) L C_2 + V_{C_B} \quad (14)$$

### 3.1.2. Boost mode

In this mode of operation, a current-controlled sliding mode controller is adopted from as stated in reference [19]. By letting  $z_1$  be the inductor current error,  $z_2$  be the output voltage error, and  $z_3$  be the integral of the sum of the inductor current and output voltage errors. Considering that the converter is operating in continuous conduction mode, the variables  $z_1$ ,  $z_2$ , and  $z_3$  can be expressed as (15);

$$\begin{cases} z_1 = i_{\text{ref-L}} - i_L \\ z_2 = V_{\text{ref}} - V_{C_A} \\ z_3 = \int (z_1 + z_2) dt \end{cases} \quad (15)$$

The instantaneous inductor's reference current,

$$i_{\text{ref-L}} = \rho (V_{\text{ref}} - V_{C_A}) \quad (16)$$

where  $\rho$  is the voltage error amplification gain,  $V_{\text{ref}}$  being the reference output voltage and  $V_{C_A}$  the voltage across the capacitor. The time derivative of  $z_1$ ,  $z_2$ , and  $z_3$  can be found as (17)-(19).

$$\dot{z}_1 = -\frac{\rho}{C_A} I_{C_A} - \frac{V_{\text{Bat}} - \bar{u} V_{C_A}}{L} \quad (17)$$

$$\dot{z}_2 = -\frac{1}{C_A} I_{C_A} \quad (18)$$

$$\dot{z}_3 = z_1 + z_2 = (\rho + 1) (V_{\text{ref}} - V_{C_A}) - i_L \quad (19)$$

where,  $\bar{u}$  is the inverse logic of  $u$  and denotes as  $\bar{u} = 1 - u$ .

Given that (6) represents the overall switching function of a sliding mode controller for this system, the sliding surface can be chosen as (20).

$$S_{\text{boost}} = \lambda_1 z_1 + \lambda_2 z_2 + \lambda_3 z_3 \quad (20)$$

with

$$S^T_{\text{boost}} = [\lambda_1, \lambda_2, \lambda_3] \quad (21)$$

By finding the time derivative of  $S_{\text{boost}}$  and solving its equal to zero, the equivalent control law becomes.

$$u_{\text{eq}} = \frac{V_{C_A} - k_2 I_{C_A} + k_1 (V_{\text{ref}} - V_{C_A}) - k_3 i_L - V_{\text{Bat}}}{V_{C_A}} \quad (22)$$

The detailed design of the control law and the calculation of its sliding coefficients can further be seen in references [14], [22]. In the boost mode of operation, the sliding mode controller needs to fulfill the existence condition, which is given by:

$$\lim_{x \rightarrow 0} S_{\text{boost}} \cdot \dot{S}_{\text{boost}} < 0,$$

hence, we can obtain the following inequalities

$$0 < V_{C_A} - k_2 I_{C_A} + k_1 (V_{\text{ref}} - V_{C_A}) - k_3 i_L - V_{\text{Bat}} < 1 \quad (23)$$

$$V_c = V_{C_A} - k_2 I_{C_A} + k_1 (V_{\text{ref}} - V_{C_A}) - k_3 i_L - V_{\text{Bat}} \quad (24)$$

$$V_{ramp} = V_{C_A} \quad (25)$$

$$\begin{cases} k_1 = \frac{\lambda_3 L(\rho+1)}{\lambda_1} \\ k_2 = \frac{L(\rho + \frac{\lambda_2}{\lambda_1})}{C_A} \\ k_3 = \frac{\lambda_3}{\lambda_1} L \end{cases} \quad (26)$$

### 3.2. Adaptive integral sliding mode controller

The goal of adaptive control is to modify the system's behavior in response to modifications in the dynamics of the process [26]. We thus incorporate an adaptive property into the traditional integral sliding mode control, since non-adaptive sliding mode control is ineffective when it comes to abrupt changes in load resistance. In this work, the adaptive sliding mode is used to further lessen the chattering impact in addition to resolving the issue of the non-adaptive sliding mode control's poor performance regarding fast changes in load. By implementing the adaptive sliding factor described in [27], [28] the design is carried out. The definitions of the adaptive sliding coefficient and sliding surface of the adaptive sliding mode are given in (27) and (28) accordingly.

$$S = \delta x_1 + \varphi_2 x_2 + \varphi_3 x_3 \quad (27)$$

where  $\varphi_2$  and  $\varphi_3$  are the sliding coefficients.

$$\delta = \frac{R}{R_c} \varphi_1 \quad (28)$$

where  $R_c \neq 0$

$$R_c = \frac{V_o}{I_o}, \text{ with } I_o \neq 0$$

where  $R$  is the nominal load resistance,  $\varphi_1$  is the sliding coefficient of the controller.  $R_c$  is the instantaneous load resistance. Detail study of the adopted adaptive control law can be seen in [28], [29]. The adaptive mechanism for the boost mode of operation is designed as in reference [30] as defined in (29), (30) and (31).

$$u = u_{eq} + u_n \quad (29)$$

$$u_n = \beta \tanh(S) \quad (30)$$

$$\beta = \frac{I_o}{V_{C_A} C_A} \quad (31)$$

### 3.3. Particle swarm optimization

Particle swarm optimization (PSO) is an optimization algorithm developed in 1995 by Dr. Eberhart and Dr. Kennedy that is based on the social behavior of fish schooling or bird flocking [31]. In recent years, researchers in a variety of power electronics converter applications have successfully used the PSO technique. This optimization strategy ensures the system will function well in a shorter length of time than prior ones [32]. This technique ensures good performance of the system within a short time as compared to other optimization techniques [31]. As stated in reference [33], the AISMC design is now expressed as an optimization problem defined in (32).

$$\text{Minimize } Q(\mu) = \sum_{t=0}^T (E(t))^2 \quad (32)$$

Subject to  $ub < \mu < lb$ .

With  $ub$  and  $lb$  being the lower and upper bounds of variables  $\mu = (\varphi_1, \varphi_2, \varphi_3)$  and  $T$  represents the start-up time for transient response. The parameters that need to be adjusted in this study are the gains and coefficients of the sliding mode controller. PSO's objective is to maximize gains for improved performance by optimizing the sliding mode controller's parameter values [34], the initial fitness of each particle in the population size was ascertained using the performance index, and the  $p_{best}$  and  $g_{best}$ , as found in reference [35], [36] were then calculated.



$$ITAE = \int_0^{\infty} |e| \quad (33)$$

Table 1 and 2 provide the parameters of the optimum values of sliding coefficients ( $\varphi_1, \varphi_2, \varphi_3$ ) for the buck mode and sliding mode controller gains ( $k_1, k_2, k_3$ ) for the boost mode, respectively, with 15 being the swarm size. To determine each particle's position and velocity in PSO, a 3-x Swarm size matrix is utilized. There can be up to 100 iterations in total. The acceleration coefficients for social and personal factors are regarded as  $C_1 = C_2 = 2$ . Simulating using MATLAB-Simulink, the performance of the optimal process is given in Figure 5. Table 2 presents the parameters of the conventional ISMC control technique and the suggested controller.

Table 1. Parameters of sliding coefficients in Buck mode

Control strategy	$\varphi_1$	$\varphi_2$	$\varphi_3$
ISMC	90.1	0.000286	177366
AISMCP SO	2.4840	4.1120e-8	1.8236e4

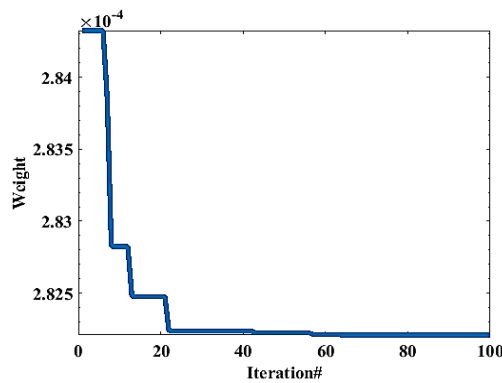


Figure 5. Iteration of the PSO algorithm

Table 2. Parameters of sliding mode controller gains in Boost mode

Control strategy	$k_1$	$k_2$	$k_2$
ISMC	750	30	4
AISMCP SO	896.01	36.203	16.032

#### 4. RESULTS AND DISCUSSION

This section discusses simulation findings using MATLAB/Simulink to support the viability of the suggested adaptive integral sliding mode control augmented by particle swarm optimization for a DC-DC converter working in bidirectional mode. The suggested controller for the buck and boost modes of a bidirectional DC-DC converter is depicted in Figure 2(a) of the schematic diagram of the system description. There is only one switching frequency, which is 20 kHz. For the step-down and step-up modes, the output voltages are 12 and 24 V, respectively, while simulating the converter at 4 ohms for buck mode and 60  $\Omega$  for boost mode. Low voltages, high voltages, and load resistance R are varied during the simulation to confirm that the suggested controller operates as intended based on transient responses. Three scenarios are derived from the simulation findings. The transient responses of the currents and voltages of the converter to step changes are examined in these circumstances. The specifications of the bidirectional half-bridge DC-DC converter are listed in Table 3 and were sourced from [22], [25].

Table 3. Simulation parameters of half-bridge bidirectional DC-DC converter

Parameters	Symbol	Value
Input voltage	$V_i$	24 V
Reference voltage	$V_{CB}$	12 V
Inductance	L	100 $\mu$ H
Capacitance	$C_A = C_B$	5 mF
Switching frequency	$f_s$	20 Hz

**4.1. Simulation results in buck mode of operation**

Scenario 1: In this scenario, the system admits a disturbance caused by an abrupt shift in input voltage from 24 to 40 V with  $t = 0.5$  s and from 40 to 15 V with  $t = 0.2$  s, respectively. The reference voltage is kept constant at 12 volts. The findings demonstrate that all three control strategies function satisfactorily in terms of robustness, with the suggested controller outperforming the two traditional methods in terms of speed, as seen in Figure 6. Figures 6(a) and 6(b) illustrate the output voltage and current, respectively. The waveform of the output voltage of the suggested controller during input voltage disturbance rejection is significantly improved upon than that of PI control and traditional integral sliding mode control, per the simulation results.

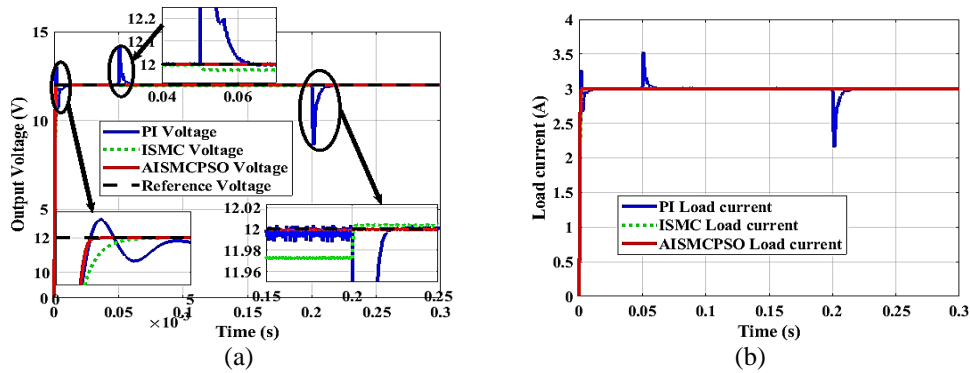


Figure 6. Simulation results of bidirectional BDC in buck mode, scenario 1 (a) output voltage and (b) load current

Scenario 2: The reference voltage in this case is adjusted by decreasing it from 12 to 8 and 10 V at intervals of 0.1 and 0.2 s, respectively, while the input voltage is set at 24 V. PI, ISMC, and the suggested controller control the converter; Figure 5 displays the output voltage and load current results. It is determined that all three control techniques have performed satisfactorily in terms of monitoring the reference voltage. Figure 7 makes it clear that the suggested controller has a quicker dynamic reaction in returning the DC-DC converter's output voltage to its matching reference values, even in spite of the sudden shift in the reference voltage. As a result, the suggested controller maximizes control-tracking accuracy compared to its conventional counterparts. The recommended controller outperformed the conventional ones in terms of speed, even though both controllers did a good job of rejecting the disturbance, as seen in Figure 7(a) and Figure 7(b). It is seen that the PI controller is overshooting.

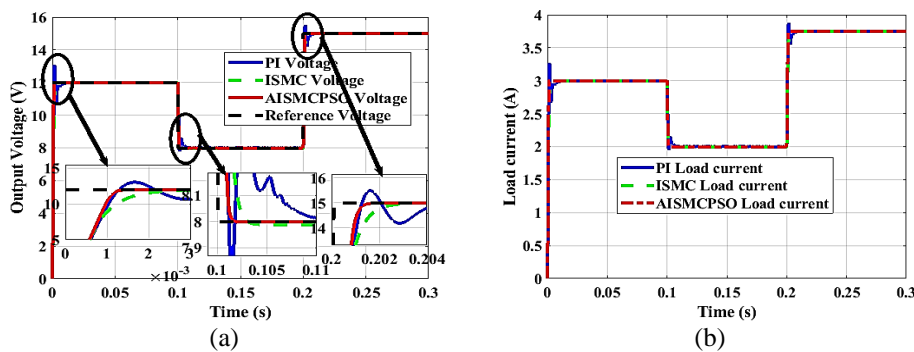


Figure 7. Simulation results of BDC in buck mode, scenario 2 (a) output voltage and (b) load current

Scenario 3: In the load resistance test, the load is reduced from 4 Ω to 2 Ω at 0.1 s and then increased to 8 Ω at 0.2 s, with a simulation period of 0.3 s. Figures 8(a) and 8(b) display the output voltage and load current waveform diagrams when the converter is under the control of PI, ISMC, and the proposed controller. From the results, it is observed that the PI control registers an overshoot when the load is increased to 8 Ω and an undershoot when the load is decreased to 2 Ω. The ISMC controller undershoots the

proposed controller. It is evident in this scenario that the proposed controller outperforms the two traditional controllers.

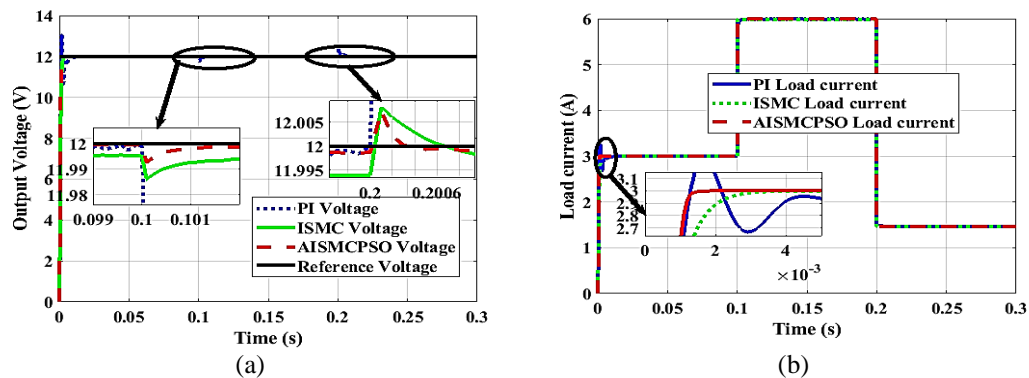


Figure 8. Simulation results of BDC in Buck mode, scenario 3 (a) output voltage and (b) load current

#### 4.2. Simulation results in boost mode of operation

Scenario 1: In the test of input voltage disturbance, the simulation time is 0.3 s. In the time interval of 0.1 and 0.2 s, the input voltage is suddenly changed from 12 to 10 V and from 10 to 15 V, respectively, to observe the behavior of the output voltage and load current. The load current and output voltage waveform diagrams under the control of the three control techniques are shown in Figure 9. According to the results shown in Figures 9(a) and 9(b), the proposed controller performs better than its conventional counterparts, with the PI controller registering undershoot and overshoot at 0.1 and 0.2 s, respectively.

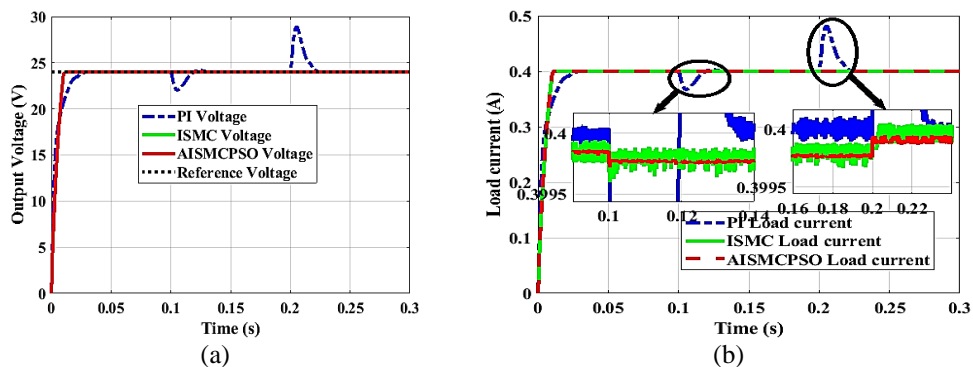


Figure 9. Simulation results of BDC in boost mode with PI, ISMC, and AISMCPSO scenario 1 (a) output voltage and (b) load current

Scenario 2: In this scenario, the output voltage reference value is changed from 24 to 30 V at  $t = 0.05$  s and from 30 to 20 V at  $t = 0.2$  s using a load resistance of  $60 \Omega$ . The results of the simulation for this situation are shown in Figure 8. With the output voltage set at its reference value, PI and ISMC both overshoot and undershoot with a steady-state inaccuracy, as shown in Figures 10(a) and 10(b). Moreover, the suggested controller does not overshoot due to the sudden shift in the reference voltage.

Scenario 3: In the load variation test, when the converter is operating in boost mode, the simulation time is 0.3 s, and the load is changed from  $60 \Omega$  to  $30 \Omega$  at the time of 0.1 s. The output voltage and current waveforms under the control of the proposed controller and classical controllers are shown in Figures 11(a) and 11(b). From the waveform, the proposed controller outperformed the other two controllers during an abrupt change of load. The proposed method is faster in tracking the reference after rejecting the disturbance, with the PI controller registering an undershoot before tracking the reference. Moreover, when the load is suddenly changed, the fluctuation of the load current and voltage under the suggested controller is also less than that of its traditional counterparts.

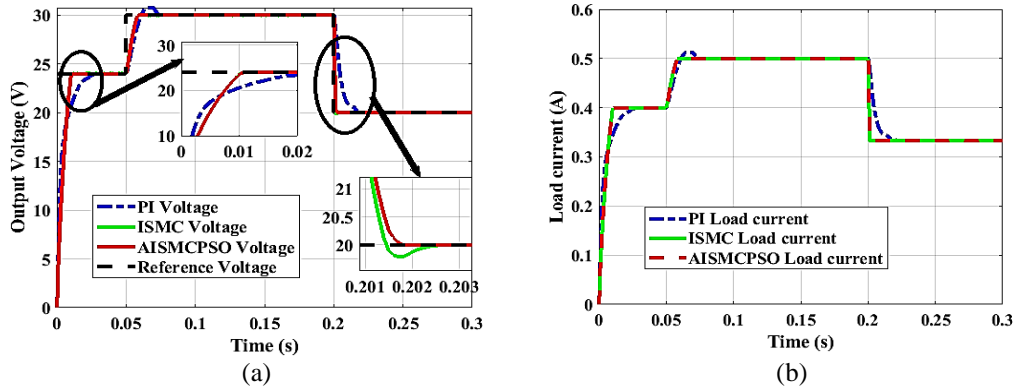


Figure 10. Simulation results of BDC in boost mode with PI, ISMC, and AISMCPSO scenario 2 (a) output voltage and (b) load current

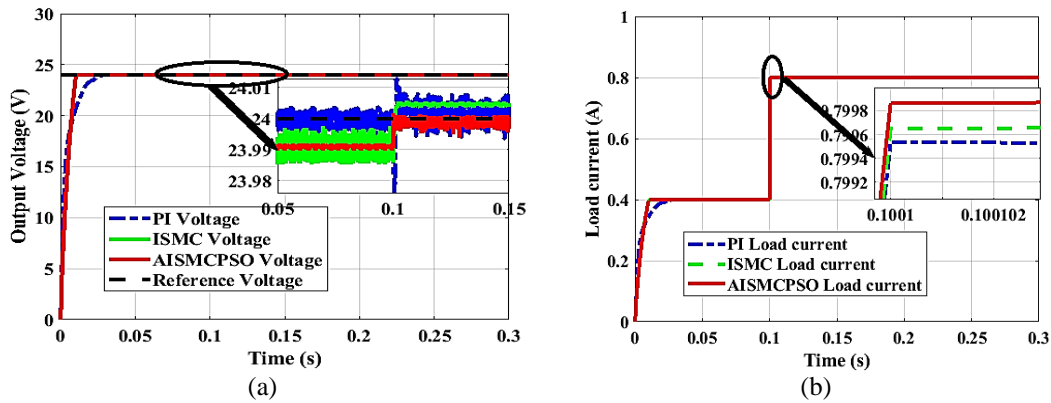


Figure 11. Simulation results of BDC in boost mode with PI, ISMC, and AISMCPSO scenario 3 (a) output voltage and (b) load current

A comparison of the suggested controller, ISMC, and PI controllers is shown in Tables 4 and 5. This indicates even more how successful the recommended controller is. Based on these findings, all three control strategies performed satisfactorily and accomplished their objectives; however, the recommended controller performed the best in terms of chattering phenomena, minimum ripples, reference tracking, and error reduction.

Table 4. Comparison of results obtained from PI, ISMC and AISMCPSO in Buck mode with  $V_{in}=24\text{ V}$ ,  $V_{ref}=12\text{ V}$ , and  $R=2\ \Omega$

Control strategy	PI	ISMC	PROPOSED
Settling time (ms)	8.4	4.6	2.6
Rise time (ms)	0.89	1.25	0.80
undershoot (%)	1.83	0.13	0.083
IAE	0.013	0.011	0.0081
ISE	0.052	0.073	0.069
SSE	0.013	0.0061	0.0014

Table 5. Comparison of results obtained from PI, ISMC and AISMCPSO in boost mode with  $V_{in}=12\text{ V}$ ,  $V_{ref}=24\text{ V}$ , and  $R=30\ \Omega$

Control strategy	PI	ISMC	PROPOSED
Settling time (ms)	1.3	0.7	0.3
Undershoot (%)	0.13	0.083	0.041
IAE	0.11	0.10	0.10
ISE	1.16	1.42	1.42
SSE	0.0052	0.0044	0.0037

## 5. CONCLUSION

In this paper, we have presented a robust and adaptive control strategy for a half-bridge bidirectional DC-DC converter, which is essential for the efficient operation of DC microgrids, energy storage systems, and electric vehicles. The proposed AISMC, enhanced by PSO, has been shown to effectively address the challenges posed by the nonlinear dynamics and external disturbances that typically affect such converters. Through comprehensive numerical simulations conducted in a MATLAB/Simulink environment, the AISMCPSO controller demonstrated superior performance compared to conventional PI and ISMC. The results highlighted significant improvements in terms of reduced settling time, minimized overshoot and undershoot, enhanced stability, and robustness under various operating conditions, including changes in input voltage, load resistance, and reference voltage. The AISMCPSO's ability to dynamically adapt to changing system parameters, thanks to the optimization provided by PSO, has proven crucial in maintaining optimal performance, reducing chattering phenomena, and ensuring reliable operation across both buck and boost modes. The significant reduction in steady-state error and the improved transient response further underscores the effectiveness of this control strategy. Overall, this research contributes a highly effective control solution for half-bridge bidirectional DC-DC converters, offering enhanced efficiency, reliability, and adaptability in dynamic and uncertain environments. This makes it a valuable tool for advancing the performance of modern DC microgrids and energy storage systems, where precision and robustness are paramount. Future work may focus on experimental validation and further refinement of the control strategy to accommodate even more complex system dynamics.





## REFERENCES

- [1] C. S. Purohit, M. Geetha, P. Sanjeevikumar, P. K. Maroti, S. Swami, and V. K. Ramachandaramurthy, "Performance analysis of DC/DC bidirectional converter with sliding mode and pi controller," *International Journal of Power Electronics and Drive Systems*, vol. 10, no. 1, pp. 357–365, Mar. 2019, doi: 10.11591/ijpeds.v10.i1.pp357-365.
- [2] H. A. Trinh *et al.*, "Robust adaptive control strategy for a bidirectional DC-DC converter based on extremum seeking and sliding mode control," *Sensors*, vol. 23, no. 1, Jan. 2023, doi: 10.3390/s23010457.
- [3] M. H. Ashfaq, J. A. Selvaraj, and N. A. Rahim, "Control strategies for bidirectional DC-DC converters: an overview," *IOP Conference Series: Materials Science and Engineering*, vol. 1127, no. 1, Mar. 2021, doi: 10.1088/1757-899x/1127/1/012031.
- [4] S. Farajdadian, A. Hajizadeh, and M. Soltani, "Recent developments of multiport DC/DC converter topologies, control strategies, and applications: A comparative review and analysis," *Energy Reports*, vol. 11, pp. 1019–1052, Jun. 2024, doi: 10.1016/j.egyr.2023.12.054.
- [5] S. A. Gorji, H. G. Sahebi, M. Ektesabi, and A. B. Rad, "Topologies and control schemes of bidirectional DC–DC power converters: an overview," *IEEE Access*, vol. 7, pp. 117997–118019, 2019, doi: 10.1109/ACCESS.2019.2937239.
- [6] S. Mahalakshmi, K. Vasanth, and P. J. R. Muniraj, "Impact factor: 4.295 sliding mode controller with modified sliding function of buck converter DC-DC," *International Journal of Advance Research*, 2017.
- [7] K. R. Bharath, H. Choutapalli, and P. Kanakasabapathy, "Control of bidirectional DC-DC converter in renewable based DC microgrid with improved voltage stability," *International Journal of Renewable Energy Research*, vol. 8, no. 2, pp. 871–877, 2018, doi: 10.20508/ijrer.v8i2.7509.g7374.
- [8] T. A. Odhafa, I. A. Abed, and A. A. Obed, "Controlling of boost converter by proportional integral controller," *International Transaction Journal of Engineering*, vol. 12, no. 4, pp. 1–8, 2021.
- [9] V. Viswanatha, R. V. S. Reddy, and Rajeswari, "Characterization of analog and digital control loops for bidirectional buck–boost converter using PID/PIDN algorithms," *Journal of Electrical Systems and Information Technology*, vol. 7, no. 1, Apr. 2020, doi: 10.1186/s43067-020-00015-6.
- [10] V. Viswanatha, R. V. S. Reddy, and Rajeswari, "Closed loop control of bidirectional buck-boost converter," *EasyChair Preprint*, 2022.
- [11] A. S. Samosir, T. Sutikno, and L. Mardiyah, "Simple formula for designing the PID controller of a DC-DC buck converter," *International Journal of Power Electronics and Drive Systems*, vol. 14, no. 1, pp. 327–336, Mar. 2023, doi: 10.11591/ijpeds.v14.i1.pp327-336.
- [12] P. Pany, R. K. Singh, and R. K. Tripathi, "Bidirectional DC-DC converter fed drive for electric vehicle system," *International Journal of Engineering, Science and Technology*, vol. 3, no. 3, Jul. 2011, doi: 10.4314/ijest.v3i3.68426.
- [13] H. Cheng, Y. Guo, Z. Ma, and S. Bai, "Design of half-bridge bidirectional DC-DC converter control loop," *Journal of Physics: Conference Series*, vol. 1894, no. 1, p. 12004, Apr. 2021, doi: 10.1088/1742-6596/1894/1/012004.
- [14] M. A. F. Al-Qaisi, M. A. Shehab, A. Al-Gizi, and M. Al-Saadi, "High performance DC/DC buck converter using sliding mode controller," *International Journal of Power Electronics and Drive Systems*, vol. 10, no. 4, pp. 1806–1814, Dec. 2019, doi: 10.11591/ijpeds.v10.i4.pp1806-1814.
- [15] T. Waghmare and P. Chaturvedi, "A higher-order sliding mode controller's super twisting technique for a DC–DC converter in photovoltaic applications," *Energy Reports*, vol. 9, pp. 581–589, Oct. 2023, doi: 10.1016/j.egyr.2023.05.054.
- [16] L. Wang, T. Miao, X. Liu, and S. Liu, "Sliding mode control of Bi-directional DC/DC converter in DC microgrid based on exact feedback linearization," *Wseas Transactions on Circuits and Systems*, vol. 19, pp. 206–211, Oct. 2020, doi: 10.37394/23201.2020.19.23.
- [17] S. Liu *et al.*, "Application of an improved STSMC method to the bidirectional DC–DC converter in photovoltaic DC microgrid," *Energies*, vol. 15, no. 5, Feb. 2022, doi: 10.3390/en15051636.
- [18] F. Errahimi, N. Es sbai, Z. El Idrissi, and Y. Cheddadi, "Robust integral sliding mode controller design of a bidirectional DC charger in PV-EV charging station," *International Journal of Digital Signals and Smart Systems*, vol. 5, no. 2, 2021, doi: 10.1504/ijdss.2021.10036181.
- [19] A. Safari and H. Ardi, "Sliding mode control of a bidirectional buck/boost DC-DC converter with constant switching frequency," *Iranian Journal of Electrical and Electronic Engineering*, vol. 14, no. 1, pp. 69–84, 2018, doi: 10.22068/IJEE.14.1.69.





- [20] R. Pramanik and B. B. Pati, "Modelling and control of a non-isolated half-bridge bidirectional DC-DC converter with an energy management topology applicable with EV/HEV," *Journal of King Saud University - Engineering Sciences*, vol. 35, no. 2, pp. 116–122, Feb. 2023, doi: 10.1016/j.jksues.2021.03.004.
- [21] P. Sivaraman, T. Logeswaran, J. S. Sakthi Surya Raj, and S. Boopathimanikandan, "Design and analysis of sliding mode control for battery charging applications," *IOP Conference Series: Materials Science and Engineering*, vol. 995, no. 1, p. 12002, Nov. 2020, doi: 10.1088/1757-899X/995/1/012002.
- [22] K. Kanthi Mathew and D. M. Abraham, "PWM-based sliding mode current controller for bidirectional DC-DC converters in electric vehicles," in *Proceedings of 2020 IEEE International Conference on Power, Instrumentation, Control and Computing, PICC 2020*, Dec. 2020, pp. 1–6, doi: 10.1109/PICC51425.2020.9362431.
- [23] S. V. Teja, T. N. Shanavas, and S. K. Patnaik, "Modified PSO based sliding-mode controller parameters for buck converter," in *2012 IEEE Students' Conference on Electrical, Electronics and Computer Science*, Mar. 2012, pp. 1–4, doi: 10.1109/SCEECS.2012.6184759.
- [24] S. C. Tan, Y. M. Lai, and C. K. Tse, "A unified approach to the design of PWM-based sliding-mode voltage controllers for basic DC-DC converters in continuous conduction mode," *IEEE Transactions on Circuits and Systems I: Regular Papers*, vol. 53, no. 8, pp. 1816–1827, Aug. 2006, doi: 10.1109/TCSI.2006.879052.
- [25] J. Cao, Q. Chen, L. Zhang, and S. Quan, "Sliding mode control of bidirectional DC/DC converter," in *2018 33rd Youth Academic Annual Conference of Chinese Association of Automation (YAC)*, May 2018, pp. 717–721, doi: 10.1109/YAC.2018.8406465.
- [26] L. T. Rasheed, "Performance of the adaptive sliding mode control scheme for output voltage control of the DC/DC buck converter system," *IOP Conference Series: Materials Science and Engineering*, vol. 881, no. 1, Jul. 2020, doi: 10.1088/1757-899X/881/1/012118.
- [27] S. C. Tan, Y. M. Lai, C. K. Tse, and M. K. H. Cheung, "An adaptive sliding mode controller for buck converter in continuous conduction mode," in *Conference Proceedings - IEEE Applied Power Electronics Conference and Exposition - APEC*, 2004, vol. 3, pp. 1395–1400, doi: 10.1109/APEC.2004.1296046.
- [28] F. Tahri, A. Tahri, and S. Flazi, "Sliding mode control for DC-DC buck converter," in *Third International Conference on Power Electronics and Electrical Drives ICPEED*, 2014, pp. 1–5.
- [29] G. Mustafa, F. Ahmad, R. Zhang, E. U. Haq, and M. Hussain, "Adaptive sliding mode control of buck converter feeding resistive and constant power load in DC microgrid," *Energy Reports*, vol. 9, pp. 1026–1035, Mar. 2023, doi: 10.1016/j.egy.2022.11.131.
- [30] A. J. Mehta and B. B. Naik, "Adaptive sliding mode controller with modified sliding function for DC-DC boost converter," in *2014 IEEE International Conference on Power Electronics, Drives and Energy Systems (PEDES)*, Dec. 2014, pp. 1–5, doi: 10.1109/PEDES.2014.7042009.
- [31] N. Mustafa and F. H. Hashim, "Design of a predictive PID controller using particle swarm optimization," *International Journal of Electronics and Telecommunications*, pp. 737–743, Jul. 2020, doi: 10.24425/ijet.2020.134035.
- [32] A. Debnath, T. O. Olowu, S. Roy, I. Parvez, and A. Sarwat, "Particle swarm optimization-based PID controller design for DC-DC buck converter," in *2021 North American Power Symposium, NAPS 2021*, Nov. 2021, pp. 1–6, doi: 10.1109/NAPS52732.2021.9654737.
- [33] P. N. Menon and A. R., "A practical particle swarm optimized sliding mode controller for an AC-DC boost converter," *International Journal of Scientific and Engineering Research*, vol. 5, no. 8, pp. 320–325, 2014.
- [34] V. N. Ogar, S. Hussain, and K. A. A. Gamage, "Load frequency control using the particle swarm optimisation algorithm and PID controller for effective monitoring of transmission line," *Energies*, vol. 16, no. 15, Aug. 2023, doi: 10.3390/en16155748.
- [35] N. A. Azli, N. M. Nayan, and S. M. Ayob, "Particle swarm optimisation and its applications in power converter systems," *International Journal of Artificial Intelligence and Soft Computing*, vol. 3, no. 4, 2013, doi: 10.1504/ijaisc.2013.056848.
- [36] H. Abderrezek and M. N. Harmas, "PSO based adaptive terminal sliding mode controllers for a DC-DC converter," *International Journal of Computer Theory and Engineering*, vol. 6, no. 4, pp. 302–306, 2014, doi: 10.7763/ijcte.2014.v6.879.

## BIOGRAPHIES OF AUTHORS






**Julius Derghe Cham**     is a Ph.D. student in the Laboratory of Technology and Applied Science at the University of Douala. He received his Dipet 2, M.Sc., and M.Eng. degrees in electrical engineering from the University of Bamenda, Douala, and Buea in 2015, 2020, and 2021, respectively. His research interests include the fields of power electronics, renewable energy, artificial intelligence, and non-linear control. He can be contacted at email: julius.cham@yahoo.com.






**Francis Léline Djanna Koffi**     is an academic researcher at the University of Douala, specializing in environmental science and biomass ecology. With a strong record of scholarly contributions, he has participated in over 30 conferences and has authored more than 30 peer-reviewed scientific publications. Djanna has also played a significant role in academic mentorship, supervising 30 master's and 5 Ph.D. thesis. Currently, he serves as the Head of the Division of Internships, where he is responsible for overseeing permanent training and fostering relationships with professional skills networks. He can be contacted via email: djannaf@yahoo.com.



**Alexandre Teplaira Boum**    is full professor in electrical engineering, holder of master's degree in electrical engineering and a Ph.D. in process control. His domain of interest is process control, optimization, embedded systems, smart grid, supervisory control. He can be contacted at email: boumat2002@yahoo.fr.



**Ambe Harrison**    is an independent researcher affiliated with the Department of Electrical and Electronics Engineering at the College of Technology (COT), University of Buea, Cameroon. His is currently interested in renewable energy development studies (Africa), real-time climatic resource estimation and optimization of PV systems, solar emulation, and nonlinear control. Harrison has authored/co-authored over 25 papers and reviewed more than 60 scientific articles. He is the founder of the Africa renewable energy hub (AREH), an initiative dedicated to advancing renewable energy development in Africa through research and communication. He can be contacted at email ambe.harrison@ubuea.cm.